British Journal of Pharmacology (2004) 142, 317–322
www.nature.com/bjp

Schaffer collateral and perforant path inputs activate different subtypes of NMDA receptors on the same CA1 pyramidal cell

[1]Elda Arrigoni & *,[2]Robert W. Greene

[1]Department of Neurology, Beth Israel Deaconess Medical Center & Harvard Medical School, Boston, MA, U.S.A. and [2]Department of Psychiatry, University of Texas Southwestern Medical Center & Dallas VA Medical Center, 4500 Lancaster Rd, 116A, Dallas, TX 75216, U.S.A.

1 The two major inputs to CA1 pyramidal neurons, the perforant pathway (PP) that terminates on distal dendrites and the Schaffer collaterals (SCH) that terminate on proximal dendrites, activate both AMPA and *N*-methyl-D-aspartate (NMDA) receptors.

2 In an *in vitro* slice preparation, the pharmacologically isolated NMDA receptor-mediated excitatory postsynaptic currents (EPSCs) (NMDA-EPSCs) of either pathway can be selectively activated onto a single CA1 pyramidal neuron.

3 Analysis of the decay phase of PP and SCH NMDA-EPSCs revealed no significant difference in their time constants, suggesting no apparent different distribution in NR2-subunit composition in the NMDA receptors (NMDAR) activated by the two synaptic inputs.

4 However, application of the NR2B-selective antagonist, ifenprodil, differently affected the NMDA-EPSCs activated by the PP and SCH inputs. The reduction of the PP responses was only 30% compared to 75% for the SCH responses.

5 In addition, for both pathways, the ifenprodil-insensitive component of the NMDA-EPSCs had significantly more rapid decay kinetics than those prior to application of ifenprodil.

6 Our results show a greater NR2B subunit contribution to the NMDA component of the SCH EPSC, compared to the NMDA component of the PP EPSC and that in single CA1 pyramidal neurons NMDA composition is anatomically specific to the afferent input.
British Journal of Pharmacology (2004) **142,** 317–322. doi:10.1038/sj.bjp.0705744

Keywords: Ifenprodil; NR2B subunit; Schaffer collateral; perforant pathway; NMDA receptor-mediated EPSC; EPSC decay kinetics; whole-cell patch-clamp

Abbreviations: ACSF, artificial cerebrospinal fluid; APV, aminophosphonovaleric acid; CGP55845, 3-N1-S-3, 4-dichlorophenyl ethyl amino-2-S-hydroxypropyl-P-benzyl-phosphinic acid; NBQX, 2,3-dihydroxy-6-nitro-7-sulfamoyl-benzo-(F)-quinoxaline; NMDA, *N*-methyl-d-aspartate; NMDA-EPSC, *N*-methyl-d-aspartate receptor-mediated excitatory postsynaptic currents; NMDAR, *N*-methyl-d-aspartate receptor; PP, perforant pathway; QX314, lidocaine *N*-ethyl bromide; SCH, Schaffer collaterals

Introduction

The *N*-methyl-D-aspartate (NMDA) receptors are glutamate-activated cation channels characterized by permeability to Ca^{2+}, a voltage-dependent block by Mg^{2+} and the presence of many modulatory sites. NMDA receptors (NMDAR) are heteromeric subunit complexes composed of the obligatory NR1 subunit (Forrest *et al*., 1994) and at least one copy of NR2A, NR2B, NR2C or NR2D (Kutsuwada *et al*., 1992; Monyer *et al*., 1992). The NR1 subunit exists in eight isoforms generated from alternative splicing of a single gene, is essential for the channel activity and is expressed ubiquitously in the central nervous system. In contrast, NR2A-D subunits are transcribed from separate genes, show developmental and regional expression and they determine pharmacological and kinetic properties of the NMDARs (McBain & Mayer, 1994; Dingledine *et al*., 1999).

The heteromeric subunit combinations of NMDAR are not equally distributed in the central nervous system. They can progressively change during development (Cull-Candy *et al*., 2001) or, even within the same neuron, different NMDAR subunit compositions can be observed between specific inputs (Ito *et al*., 2000; Kawakami *et al*., 2003; Kumar & Huguenard, 2003). Owing to the topographic organization of their synaptic inputs, CA1 pyramidal neurons are a useful model for studying the receptor composition of specific inputs, and may offer the opportunity to test for a possible relationship between the particular synaptic input and NMDAR subunit composition. It is known that in the CA1 region of the adult hippocampus, NR2A and NR2B mRNAs predominate in pyramidal cells, while NR2C and NR2D mRNAs predominate in nonpyramidal cells (Monyer *et al*., 1994). CA1 pyramidal neurons receive two anatomically segregated glutamatergic inputs, the perforant pathway (PP), originating in layer 3 of the entorhinal cortex and terminating on distal CA1 dendrites in the stratum lacunosum moleculare and the Schaffer collaterals (SCH), originating from CA3 pyramidal neurons and terminating on proximal CA1 dendrites in the stratum radiatum (Steward, 1976). Previous *in vitro* studies have shown

*Author for correspondence:
E-mail: ROBERTW.GREEN@UTSouthwestern.edu

that these two pathways can be separately activated and further that they respond differently to muscarinic, $GABA_B$ and monoamine receptor activations (Ault and Nadler, 1982; Colbert & Levy, 1992; Hasselmo & Schnell, 1994; Nejtek & Dahl, 1997; Otmakhova & Lisman, 1999; 2000). The input specificity of these effects is more likely due to differences in the distribution of presynaptic receptors in the PP *versus* SCH terminals. More recent work has compared the properties of the NMDA and AMPA receptors that in CA1 neurons are separately activated by the PP and the SCH inputs (Otmakhova & Lisman, 2002). Using a similar preparation, here we characterized the subunit composition of the NMDAR mediating the responses activated by each of these two inputs.

Methods

Slice preparation

Long-evans (7–8 weeks) rats were deeply anesthetized with isoflurane, decapitated, their brains removed, and the hippocampus dissected and cut in transverse slices (400-μm thick). Part of the dentate gyrus and the CA3 field were removed from the slices in order to interrupt the trisynaptic pathway dentate→CA3→CA1 (Colbert & Levy, 1992; Otmakhova & Lisman, 1999). Slices were then incubated at room temperature in artificial cerebrospinal fluid (ACSF) containing (in mM): NaCl, 124; KCl, 2; KH_2PO_4, 3; $MgCl_2$, 1.3; $CaCl_2$, 2.5; $NaHCO_3$, 26; glucose, 10 (pH 7.35; 315–320 mOsm when gassed with O_2 95% and CO_2 5%) for about 1 h before the recordings started.

Whole-cell recordings

Whole-cell patch-clamp recordings were performed in voltage-clamp mode using an Axopatch-1D amplifier (Axon Instruments, Foster City, CA, U.S.A.). Data acquisition and analysis were conducted with a Digidata 1200B interface and Clampex 8.0 software (Axon Instruments, Foster City, CA, U.S.A.). Signals were low-pass filtered at 2 kHz and digitized at 5 or 10 kHz. Individual slices were recorded while submerged in ACSF (flow rate 1.8 ml min^{-1}) at 32°C. Patch electrodes were prepared from borosilicate glass tubing (O.D. 1.5 mm; I.D. 0.86, with filament) with a P97 pipette puller (Sutter Instrument, Novato, CA, U.S.A.). Electrodes (7–10 MΩ) were filled with a recording solution containing (in mM): 120 K-gluconate, 10 KCl, 3 $MgCl_2$, 10 HEPES, 2 MgATP, 0.2 NaGTP (pH 7.2 adjusted with KOH; 280 mOsm) and 1 mM lidocaine *N*-ethyl bromide (QX314; Tocris, Ellisville, MO, U.S.A.) and 2 mM D890 (Knoll, Ludwghsafen, Germany) were added to block the voltage-dependent soma-dendritic currents and to improve the voltage control of the NMDA-EPSCs (Kovalchuk *et al*., 2000; Otmakhova *et al*., 2002). Series resistance was 9–20 MΩ and was monitored at regular intervals throughout the course of the experiments with voltage pulses (−5 mV; 20 ms). Data were discarded if the series resistance changed by more than 20% during an experiment. The PP and SCH inputs were activated by using two stimulating bipolar electrodes placed in the stratum moleculare of the subiculum and in the stratum radiatum, respectively. The PP and SCH inputs were activated alternately every 20 s (separated by 6 s) with a 1–50 μA, 200 μs square pulse delivered through two isolated constant-current sources, Iso-flex (A.M.P.I., Jerusalem, Israel). The stimulation trigger was controlled by Clampex 8.0 software. Pharmacologically isolated NMDA excitatory post synaptic currents (EPSCs) were obtained by recording (V_h = −60 mV) in low-Mg^{2+} ACSF (0.1 mM $MgCl_2$/3.7 mM $CaCl_2$) to maintain the same extracellular cation concentration (Bergeron *et al*., 1998) and by blocking $GABA_A$ receptors with bicuculline methiodide (20 μM), $GABA_B$ receptors (Jarolimek *et al*., 1993) with 3-N1-*S*-3,4-dichlorophenyl ethyl amino-2-*S*-hydroxypropyl-*P*-benzyl-phosphinic acid (CGP55845; 100 nM, Tocris) and AMPA receptors with 2,3-dihydroxy-6-nitro-7-sulfamoyl-benzo-(F)-quinoxaline (NBQX; 12 μM). NMDA-EPSC recordings were started after 20 min in whole-cell configuration to ensure that the intracellular blockers had time to diffuse to the distal dendrites (Otmakhova *et al*., 2002). Unless specified all reagents were purchased from Sigma-Aldrich (St. Louis, MO).

Data analysis and statistics

Current traces displayed in the figures are averages of 6–15 EPSCs. The total NMDA-EPSC-induced charge was calculated as the absolute sum of the current over time. The integrated area was set between the end of the stimulus artefact and the return to baseline of the EPSC. NMDA-EPSC rise and decay time constants were estimated by fitting with single exponential functions with a nonlinear least-squares fitting method using IGOR Pro 4.0 (WaveMetrics, Lake Oswego, OR, U.S.A.). Fit range was set between 10 and 90% of peak amplitude for the rise phase and between 90 and 10% of the peak amplitude for the decay phase. Data are presented as means ± s.e.m. and statistical significance was established by paired *t*-tests (two-tailed) with *P*-values as reported throughout the text. All the fitting results are reported together with the correlation coefficients (*R*).

Results

Pharmacological isolated PP and SCH NMDA-EPSCs recorded in single CA1 pyramidal neurons

The CA1 hippocampal pyramidal cells offer an advantage of having functionally distinct inputs that may be selectively activated by relatively large stimulation electrodes. Activation of either PP input and the SCH input evoked a fast EPSC followed by an inhibitory postsynaptic current (IPSC) in the same CA1 pyramidal neuron maintained at V_h = −60 mV (Figure 1). The IPSCs recorded at both PP and SCH synapses were completely blocked by the application of bicuculline methiodide (20 μM) and the selective $GABA_B$ antagonist CGP55845 (100 nM). Application of NBQX (12 μM) drastically reduced the amplitude of the EPSCs leaving a residual 7% of the EPSCs activated by the PP stimulation and 3% for those activated by the SCH stimulation, both were completely blocked by the application of DL-aminophosphonovaleric acid (DL-APV; 100 μM; n = 4). Thus, to isolate pharmacologically the NMDAR-mediated EPSCs (NMDA-EPSCs), recordings were made in ACSF (low Mg^{2+}) and in the presence of $GABA_A$, $GABA_B$ and AMPA receptor antagonists. Under

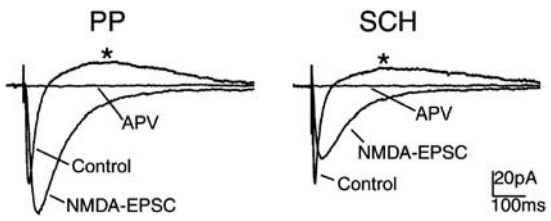

Figure 1 Isolation of NMDA receptor-mediated EPSCs. NMDA-EPSCs are recorded in a single CA1 pyramidal neuron in response to stimulations of the PP (left) and SCH (right) inputs. Recordings in normal ACSF (control) show that both PP and SCH activations evoke in the CA1 neuron a fast AMPA receptor-mediated EPSC followed by a $GABA_B$ receptor-mediated IPSC (asterisks). To obtain isolated NMDA-EPSCs, recordings are performed at $V_h = -60$ mV, in ACSF (low Mg^{2+}), bicuculline methiodide (20 μM), CGP55845 (100 nM) and NBQX (12 μM). The NMDA-EPSCs are completely blocked by the application of DL-APV (100 μM).

these conditions, isolated NMDA-EPSCs at both PP and SCH synapses were completely abolished by DL-APV ($n = 10$). At the start of each experiment, the stimulation strengths were adjusted so that the EPSC amplitudes were approximately equal for both pathways. However, when ACSF (low Mg^{2+}) was applied and $GABA_A$, $GABA_B$ and AMPA receptors were blocked, the same stimulation intensity evoked larger NMDA-EPSCs at the PP synapses (Figure 1). The apparent ratios $NMDA_{(\text{in low Mg})}/AMPA + NMDA_{(\text{in normal ACSF})}$ were 1.63 ± 0.2 at the PP and 0.71 ± 0.08 at the SCH synapses ($P < 0.01$, paired t-test; $n = 16$). These results are consistent with previous work where, under similar experimental conditions, a higher NMDA component at the PP *versus* the SCH synapses was reported (Otmakhova *et al*., 2002).

Rise and decay kinetics of PP and SCH NMDA-EPSCs

To examine the kinetics of the NMDA component of the EPSCs, the strength of the PP stimulation was decreased to bring the PP NMDA-EPSC amplitude to approximately the same as the SCH NMDA-EPSC. Kinetics of rise phases of PP and SCH NMDA-EPSCs were determined by best fit with single exponential functions. Rise phases at the PP synapses were significantly slower: 28.1 ± 2.5 ms ($R = 0.9727 \pm 0.0022$) for PP NMDA-EPSCs and 17.9 ± 1.2 ms ($R = 0.9757 \pm 0.0034$) for SCH NMDA-EPSCs ($P = 0.004$, paired t-test; $n = 16$). This difference reflects, in large part, the greater electronic distance of the PP input (Hausser & Roth, 1997). The deactivation of NMDA-EPSCs has often been fit with double exponentials; however, single weighted (Stocca & Vicini, 1998; Chapman *et al*., 2003) as well as single exponential (Hestrin, 1992; Kumar & Huguenard, 2003) functions have also been reported. We found that increasing the order did not improve the fit and did not yield independent exponential terms. Kinetics of decay phases of PP and SCH NMDA-EPSCs were therefore determined by best fit with single exponential functions. Analysis of the decay phase of PP and SCH NMDA-EPSCs revealed no significant difference in their time constants. NMDA-EPSC decay time constants were 90.5 ± 6.3 ms ($R = 0.9685 \pm 0.0029$) for the PP and 87.7 ± 6.8 ms ($R = 0.9659 \pm 0.0045$) for the SCH pathway ($P = 0.6$, paired t-test; $n = 16$).

NR2B content of the NMDARs at the PP and SCH synapses

To determine whether there was a difference in NR2B-containing NMDAR compositions at the PP and SCH synapses, we tested the effects of ifenprodil on the PP and SCH NMDA-EPSCs in 10 neurons. Ifenprodil is a noncompetitive, activity-dependent and voltage-independent antagonist of NR2B subunit containing NMDARs (Williams, 1993; 1995). Ifenprodil has been previously used to determine the NR2B component of NMDA synaptic inputs at concentrations between 3 and 10 μM (Lei & McBain, 2002; Kumar & Huguenard, 2003; Lopez de Armentia & Sah, 2003). Ifenprodil dose–response studies on both recombinant (Williams, 1993; Mott *et al*., 1998) and native (Kirson & Yaari, 1996) NMDARs have shown that in this concentration range, ifenprodil is a selective antagonist for the NR2B subunit containing NMDARs. We tested ifenprodil at 10 μM concentration on both PP and SCH NMDA-EPSCs. Within single CA1 pyramidal neurons, the proportion of ifenprodil-sensitive components of the NMDA-EPSCs (NR2B mediated) was significantly higher at the SCH synapses compared to the PP synapses (Figures 2a, b and 3). Ifenprodil sensitivity at both PP and SCH inputs was established as a reduction of the EPSC, total recovered charge, measured as the area of the EPSC. The EPSC recovered charge is the most accurate method available for characterizing EPSC magnitude (Hausser & Roth, 1997), and has been successfully used to analyze the PP input on the distal dendrite (Otmakhova *et al*., 2002). While the peak of the synaptic currents is attenuated with increasing electrotonic

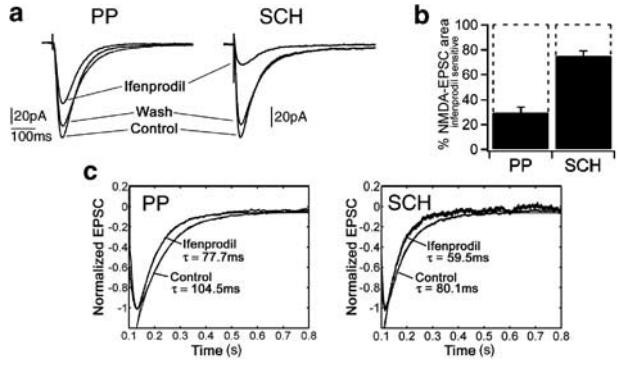

Figure 2 Ifenprodil effects on NMDA-EPSC evoked charge and decay kinetics. (a) Example of ifenprodil effects on NMDA-EPSCs recorded in a single CA1 pyramidal neuron evoked by PP (left) and SCH (right) stimulations. In this neuron ifenprodil (10 μM) reduces the PP NMDA-EPSC charge by 35% (control 12.15 pA × ms; ifenprodil 7.38 pA × ms) and the SCH NMDA-EPSC charge by 77% (control 11.31 pA × ms; ifenprodil 2.56 pA × ms). (b) Averaged data from ifenprodil-mediated inhibition of the NMDA-EPSC charge. Ifenprodil reduces the PP NMDA-EPSC charge by 29.6 ± 4.4% and SCH NMDA-EPSC charge by 75.1 ± 4.07% ($P < 0.01$, paired t-test; $n = 10$). Errors bars represent the s.e.m. (c) Ifenprodil effect on the kinetics of NMDA-EPSC decay phase. The ifenprodil-insensitive component of the NMDA-EPSCs activated by either PP and SCH pathways have more rapid decay kinetics compared to the corresponding NMDA-EPSCs measured in control. The traces are the result of averaging peak-aligned, normalized NMDA-EPSCs recorded in five neurons. The decay phase is best fit with a single exponential equation which is shown superimposed on the average NMDA-EPSC. Correlation coefficients (R) for PP were: 0.9805 (control) and 0.9852 (ifenprodil); and for SCH: 0.9771 (control) and 0.9659 (ifenprodil).

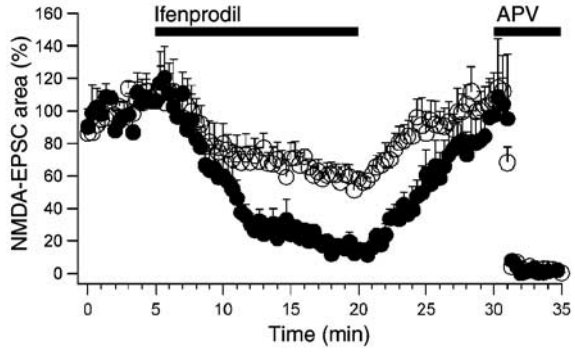

Figure 3 Time course of the effect of ifenprodil on NMDA-EPSC charge. Average responses of four CA1 pyramidal neurons to the application of ifenprodil (10 μM) and DL-APV (100 μM) on NMDA-EPSCs evoked by stimulation of both PP (empty dots) and SCH (filled dots). The percentage of NMDA-EPSC charge is calculated by taking the mean NMDA-EPSC charge during the first 5 min (control) as 100%.

distances, the synaptic charge is less affected and is relatively independent of the kinetics of the synaptic conductance (Hausser & Roth, 1997). Ifenprodil reduced the PP NMDA-EPSC charge by $29.6 \pm 4.4\%$ and SCH NMDA-EPSC charge by $75.1 \pm 4.07\%$ ($P < 0.01$, paired t-test; $n = 10$). The time course of ifenprodil effects on the EPSC evoked charge was monitored in four of the neurons tested and showed a slower block compared to DL-APV (Figure 3), which is compatible with the activity-dependent property of ifenprodil action (Kew *et al*., 1996).

In addition, for both pathways, the ifenprodil-insensitive component of the NMDA-EPSCs had significantly more rapid decay kinetics than those measured on the total NMDA-EPSCs recorded prior to application of ifenprodil. The rate of decay was determined by a best fit to a single exponential. Fitting was possible for ifenprodil-insensitive currents only in five of the 10 neurons tested. In the other cases, the ifenprodil-insensitive currents for the SCH EPSCs were too small to be analyzed. Ifenprodil reduced PP and SCH NMDA-EPSC decay time constants equally (26%; $n = 5$). PP time constants measured 103.3 ± 7.9 ms in control and 73.5 ± 8.6 ms with ifenprodil. SCH time constants measured 83.7 ± 11.6 ms in control and 58.9 ± 6.7 ms with ifenprodil ($n = 5$). The average effects of ifenprodil on the decay kinetics are shown in Figure 2c where fitting was applied on averaged, peak-aligned, normalized NMDA-EPSCs.

Discussion

In summary, the NMDAR subunit composition of CA1 pyramidal cell synapses is specific to the two major CA1 inputs, the PP input and the SCH input. On the basis of the sensitivity of evoked NMDAR-dependent total charge to the NR2B-selective antagonist, ifenprodil, there is a greater contribution of the NR2B subunits to the more proximal synapses of the SCH input as compared to the more distal inputs of the PP pathway, measured on the same CA1 pyramidal neuron.

Differential NMDAR subunit composition can occur during early development such that at birth NR2B is the predominant subunit, while NR2A expression gradually increases with maturation (Monyer *et al*., 1994; Kirson & Yaari, 1996) contributing to the developmental changes in NMDA-mediated synaptic plasticity (Cull-Candy *et al*., 2001; Philpot *et al*., 2001). In mature animals within the same neuron differential NMDARs are reported between synaptic and extrasynaptic receptors (Rumbaugh & Vicini, 1999; Momiyama, 2000), and an uneven distribution of synaptic NMDAR subtypes can form a continuum (Lei & McBain, 2002) or it can be specific to the type of input (Ito *et al*., 2000; Kawakami *et al*., 2003; Kumar & Huguenard, 2003). NMDAR subtype input specific distributions were recently described in CA3 and CA1 pyramidal neurons. In CA1, NR2B subunits are evenly distributed in NMDARs activated by the CA3 input to the basilar dendrite and to the apical dendrites. However, an asymmetric difference of NMDAR subunit composition between left and right hippocampi was revealed, or possibly, induced in animals that had received a surgical lesion of commissural fibers (Kawakami *et al*., 2003). In CA3 there is a higher NR2B content in NMDARs activated by the input from the contralateral CA3 compared with those activated by the ipsilateral CA3 (Ito *et al*., 2000). Conversely, we found that on the apical dendrites of CA1 pyramidal neurons from intact adult animals a differential NMDAR subunit composition may segregate according to input, suggesting functional specificity of the NMDAR subunit composition as it correlates with functionally distinct inputs. In single CA1 pyramidal neurons differential properties of the glutamatergic-mediated response at PP and SCH inputs were also recently reported (Otmakhova *et al*., 2002). The authors show that glutamate released at the PP activates EPSCs with a larger NMDA/AMPA ratio compared to the SCH EPSCs and report that the NMDA-mediated responses were different with the PP NMDA-EPSCs exhibiting an inward rectification that persists in the absence of extracellular Mg^{2+}. Here we extend this work by characterizing the pharmacological and kinetic properties of the NMDA-EPSCs activated by these two synaptic inputs.

It has generally been assumed that at glutamatergic synapses, abundance in NR2B subunits generate EPSCs characterized by sensitivity to NR2B-selective antagonists and slow decay kinetics (Vicini *et al*., 1998; Tovar & Westbrook, 1999). However, we have found that NMDA-EPSCs activated by the SCH input are significantly more affected by the NR2B-selective antagonist ifenprodil compared to the PP NMDA-EPSCs, but we did not find them to exhibit slower decay kinetics. This result was unexpected but is not unique. Dissociation between NR2B-selective antagonist sensitivity and slow decay kinetics has been reported in the literature (Barth & Malenka, 2001). Faster NMDA-EPSC kinetics are not always associated with a replacement of NR2B by NR2A subunits, but they can reflect a NR2A expression increase (Flint *et al*., 1997; Shi *et al*., 1997). This suggests that a rearrangement of NMDA heteromers that incorporate NR2A subunits coassembled with NR2B would form NMDARs with fast kinetics (Flint *et al*., 1997; Cull-Candy *et al*., 2001) and sensitivity to NR2B-selective antagonists (Kew *et al*., 1998; Hawkins *et al*., 1999). Nevertheless, these trimeric assemblies have also been reported to lose their sensitivity to activity-dependent antagonists (Brimecombe *et al*., 1997). Based on the pharmacological properties of the responses in each pathway, and considering that in the adult hippocampus, NR2A and NR2B mRNAs predominate in pyramidal cells (Monyer *et al*.,

1994) we propose that the contribution of NR1/NR2A/NR2B heteromers in the SCH synaptic NMDARs may cause the dissociation between ifenprodil sensitivity and slow decay kinetics. Furthermore, and in accordance with the observation for recombinant NMDARs (Vicini *et al*., 1998), the decay kinetics at the SCH synapses are too fast to be attributed to the binary assembly NR1/NR2B.

An additional explanation for the discrepancy in having indistinguishable decay time constants in synapses with different ifenprodil sensitivity/NR2B content is that synapses located at different distances from the soma are filtered to varying extents. The EPSC kinetics are most distorted with increasing electrotonic distances, with greater attenuation for the faster kinetics (Hestrin *et al*., 1990; Hausser & Roth, 1997). Thus, PP NMDA-EPSC kinetics are expected to be more attenuated than those at SCH synapses. In agreement with this we found that the rise phase of the PP NMDA-EPSCs was significantly slower than the rise phase of SCH NMDA-EPSCs. Furthermore, we found the PP NMDA-EPSCs to have a decay phase slower than what we would have expected on the basis of ifenprodil sensitivity. However, exposure to ifenprodil significantly increased the decay kinetics of SCH and PP EPSCs suggesting that filtering due to membrane properties does not completely limit the rate of decay.

The NR2A/B subunit content determines many of the properties of the NMDARs (Dingledine *et al*., 1999; Loftis & Janowsky, 2003). Although we did not test for any functional difference between PP and SCH inputs, there are several functional characteristics that we predict might differentiate these two synaptic inputs according to their NR2B content. For example, recombinants containing NR1-NR2B respond to agonist application with slower time courses of deactivation, inactivation and desensitization (Krupp *et al*., 1996; Vicini *et al*., 1998; Chen *et al*., 1999), and they are 10 times more sensitive to glycine than NR1-NR2A receptors (Kutsuwada *et al*., 1992), thus alterations in local extracellular glycine concentration might have greater impact on glutamatergic inputs where NR2B composition predominates. On the other hand, open channel blockers of the NMDAR such as MK-801 act more rapidly on inputs where the NR2A receptor predominates as reported in the amygdala (Lopez de Armentia & Sah, 2003). Studies of single channels show that NR1-NR2A receptors have higher open probability than NR1-NR2B receptors, which generate NMDA-EPSCs with larger amplitude and more rapid kinetics. For equal NMDAR density, postsynaptic NR1-NR2A receptors mediate an NMDA-EPSC four-fold larger than NR1-NR2B (Chen *et al*., 1999). Along with this observation it was demonstrated that higher NR2B subunit content is associated with tolerance to excitotoxic neuronal death (Marks *et al*., 1996; Brandoli *et al*., 1998), hypoxia (Bickler *et al*., 2003) and electroconvulsive seizures induce upregulation of NR2B expression with decreased NMDA-evoked currents (Hiroi *et al*., 1998; Watkins *et al*., 1998). Finally, increased expression of NR2B subunits is associated with enhanced synaptic plasticity (Quinlan *et al*., 1999; Tang *et al*., 1999; Barth & Malenka, 2001). Thus, it is conceivable that in CA1 neurons the different NR2B content activated by the SCH and the PP might generate differences in the NMDA-mediated functional properties of these two inputs.

This work was supported by a Merit Award from The Department of Veterans Affairs to Dr Greene, by NHLBI Grant: HL60292 and by the NIMH Conti Center, MH60450-01A1. The D890 was kindly provided by Knoll, Ludwghsafen, Germany. The authors wish to thank Dr Nancy L. Chamberlin for helpful discussions and advice.

References

AULT, B. & NADLER, J.V. (1982). Baclofen selectively inhibits transmission at synapses made by axons of CA3 pyramidal cells in the hippocampal slice. *J. Pharmacol. Exp. Ther.,* **223,** 291–297.

BARTH, A.L. & MALENKA, R.C. (2001). NMDAR EPSC kinetics do not regulate the critical period for LTP at thalamocortical synapses. *Nat. Neurosci.,* **4,** 235–236.

BERGERON, R., MEYER, T.M., COYLE, J.T. & GREENE, R.W. (1998). Modulation of *N*-methyl-D-aspartate receptor function by glycine transport. *Proc. Natl. Acad. Sci. U.S.A.,* **95,** 15730–15734.

BICKLER, P.E., FAHLMAN, C.S. & TAYLOR, D.M. (2003). Oxygen sensitivity of NMDA receptors: relationship to NR2 subunit composition and hypoxia tolerance of neonatal neurons. *Neuroscience,* **118,** 25–35.

BRANDOLI, C., SANNA, A., DE BERNARDI, M.A., FOLLESA, P., BROOKER, G. & MOCCHETTI, I. (1998). Brain-derived neurotrophic factor and basic fibroblast growth factor downregulate NMDA receptor function in cerebellar granule cells. *J. Neurosci.,* **18,** 7953–7961.

BRIMECOMBE, J.C., BOECKMAN, F.A. & AIZENMAN, E. (1997). Functional consequences of NR2 subunit composition in single recombinant *N*-methyl-D-aspartate receptors. *Proc. Natl. Acad. Sci. U.S.A.,* **94,** 11019–11024.

CHAPMAN, D.E., KEEFE, K.A. & WILCOX, K.S. (2003). Evidence for functionally distinct synaptic NMDA receptors in ventromedial *versus* dorsolateral striatum. *J. Neurophysiol.,* **89,** 69–80.

CHEN, N., LUO, T. & RAYMOND, L.A. (1999). Subtype-dependence of NMDA receptor channel open probability. *J. Neurosci.,* **19,** 6844–6854.

COLBERT, C.M. & LEVY, W.B. (1992). Electrophysiological and pharmacological characterization of perforant path synapses in CA1: mediation by glutamate receptors. *J. Neurophysiol.,* **68,** 1–8.

CULL-CANDY, S., BRICKLEY, S. & FARRANT, M. (2001). NMDA receptor subunits: diversity, development and disease. *Curr. Opin. Neurobiol.,* **11,** 327–335.

DINGLEDINE, R., BORGES, K., BOWIE, D. & TRAYNELIS, S.F. (1999). The glutamate receptor ion channels. *Pharmacol. Rev.,* **51,** 7–61.

FLINT, A.C., MAISCH, U.S., WEISHAUPT, J.H., KRIEGSTEIN, A.R. & MONYER, H. (1997). NR2A subunit expression shortens NMDA receptor synaptic currents in developing neocortex. *J. Neurosci.,* **17,** 2469–2476.

FORREST, D., YUZAKI, M., SOARES, H.D., NG, L., LUK, D.C., SHENG, M., STEWART, C.L., MORGAN, J.I., CONNOR, J.A. & CURRAN, T. (1994). Targeted disruption of NMDA receptor 1 gene abolishes NMDA response and results in neonatal death. *Neuron,* **13,** 325–338.

HASSELMO, M.E. & SCHNELL, E. (1994). Laminar selectivity of the cholinergic suppression of synaptic transmission in rat hippocampal region CA1: computational modeling and brain slice physiology. *J. Neurosci.,* **14,** 3898–3914.

HAUSSER, M. & ROTH, A. (1997). Estimating the time course of the excitatory synaptic conductance in neocortical pyramidal cells using a novel voltage jump method. *J. Neurosci.,* **17,** 7606–7625.

HAWKINS, L.M., CHAZOT, P.L. & STEPHENSON, F.A. (1999). Biochemical evidence for the co-association of three *N*-methyl-D-aspartate (NMDA) R2 subunits in recombinant NMDA receptors. *J. Biol. Chem.,* **274,** 27211–27218.

HESTRIN, S. (1992). Developmental regulation of NMDA receptor-mediated synaptic currents at a central synapse. *Nature,* **357,** 686–689.

HESTRIN, S., NICOLL, R.A., PERKEL, D.J. & SAH, P. (1990). Analysis of excitatory synaptic action in pyramidal cells using whole-cell recording from rat hippocampal slices. *J. Physiol.,* **422,** 203–225.

HIROI, N., MAREK, G.J., BROWN, J.R., YE, H., SAUDOU, F., VAIDYA, V.A., DUMAN, R.S., GREENBERG, M.E. & NESTLER, E.J. (1998). Essential role of the fosB gene in molecular, cellular, and behavioral actions of chronic electroconvulsive seizures. *J. Neurosci.,* **18,** 6952–6962.

ITO, I., KAWAKAMI, R., SAKIMURA, K., MISHINA, M. & SUGIYAMA, H. (2000). Input-specific targeting of NMDA receptor subtypes at mouse hippocampal CA3 pyramidal neuron synapses. *Neuropharmacology,* **39,** 943–951.

JAROLIMEK, W., DEMMELHUBER, J., BIJAK, M. & MISGELD, U. (1993). CGP 55845A blocks baclofen, gamma-aminobutyric acid and inhibitory postsynaptic potassium currents in guinea pig CA3 neurons. *Neurosci. Lett.,* **154,** 31–34.

KAWAKAMI, R., SHINOHARA, Y., KATO, Y., SUGIYAMA, H., SHIGEMOTO, R. & ITO, I. (2003). Asymmetrical allocation of NMDA receptor epsilon2 subunits in hippocampal circuitry. *Science,* **300,** 990–994.

KEW, J.N., RICHARDS, J.G., MUTEL, V. & KEMP, J.A. (1998). Developmental changes in NMDA receptor glycine affinity and ifenprodil sensitivity reveal three distinct populations of NMDA receptors in individual rat cortical neurons. *J. Neurosci.,* **18,** 1935–1943.

KEW, J.N., TRUBE, G. & KEMP, J.A. (1996). A novel mechanism of activity-dependent NMDA receptor antagonism describes the effect of ifenprodil in rat cultured cortical neurones. *J. Physiol.,* **497** (Part 3), 761–772.

KIRSON, E.D. & YAARI, Y. (1996). Synaptic NMDA receptors in developing mouse hippocampal neurones: functional properties and sensitivity to ifenprodil. *J. Physiol.,* **497** (Part 2), 437–455.

KOVALCHUK, Y., EILERS, J., LISMAN, J. & KONNERTH, A. (2000). NMDA receptor-mediated subthreshold Ca(2+) signals in spines of hippocampal neurons. *J. Neurosci.,* **20,** 1791–1799.

KRUPP, J.J., VISSEL, B., HEINEMANN, S.F. & WESTBROOK, G.L. (1996). Calcium-dependent inactivation of recombinant *N*-methyl-D-aspartate receptors is NR2 subunit specific. *Mol. Pharmacol.,* **50,** 1680–1688.

KUMAR, S.S. & HUGUENARD, J.R. (2003). Pathway-specific differences in subunit composition of synaptic NMDA receptors on pyramidal neurons in neocortex. *J. Neurosci.,* **23,** 10074–10083.

KUTSUWADA, T., KASHIWABUCHI, N., MORI, H., SAKIMURA, K., KUSHIYA, E., ARAKI, K., MEGURO, H., MASAKI, H., KUMANISHI, T., ARAKAWA, M. & MISHINA, M (1992). Molecular diversity of the NMDA receptor channel. *Nature,* **358,** 36–41.

LEI, S. & MCBAIN, C.J. (2002). Distinct NMDA receptors provide differential modes of transmission at mossy fiber–interneuron synapses. *Neuron,* **33,** 921–933.

LOFTIS, J.M. & JANOWSKY, A. (2003). The *N*-methyl-d-aspartate receptor subunit NR2B: localization, functional properties, regulation, and clinical implications. *Pharmacol. Ther.,* **97,** 55–85.

LOPEZ DE ARMENTIA, M. & SAH, P. (2003). Development and subunit composition of synaptic NMDA receptors in the amygdala: NR2B synapses in the adult central amygdala. *J. Neurosci.,* **23,** 6876–6883.

MARKS, J.D., FRIEDMAN, J.E. & HADDAD, G.G. (1996). Vulnerability of CA1 neurons to glutamate is developmentally regulated. *Brain Res. Dev. Brain Res.,* **97,** 194–206.

MCBAIN, C.J. & MAYER, M.L. (1994). *N*-methyl-D-aspartic acid receptor structure and function. *Physiol. Rev.,* **74,** 723–760.

MOMIYAMA, A. (2000). Distinct synaptic and extrasynaptic NMDA receptors identified in dorsal horn neurones of the adult rat spinal cord. *J. Physiol.,* **523** (Part 3), 621–628.

MONYER, H., BURNASHEV, N., LAURIE, D.J., SAKMANN, B. & SEEBURG, P.H. (1994). Developmental and regional expression in the rat brain and functional properties of four NMDA receptors. *Neuron,* **12,** 529–540.

MONYER, H., SPRENGEL, R., SCHOEPFER, R., HERB, A., HIGUCHI, M., LOMELI, H., BURNASHEV, N., SAKMANN, B. & SEEBURG, P.H. (1992). Heteromeric NMDA receptors: molecular and functional distinction of subtypes. *Science,* **256,** 1217–1221.

MOTT, D.D., DOHERTY, J.J., ZHANG, S., WASHBURN, M.S., FENDLEY, M.J., LYUBOSLAVSKY, P., TRAYNELIS, S.F. & DINGLEDINE, R. (1998). Phenylethanolamines inhibit NMDA receptors by enhancing proton inhibition. *Nat. Neurosci.,* **1,** 659–667.

NEJTEK, V. & DAHL, D. (1997). Pathway specificity of l-isoproterenol indicates beta-adrenergic modulation of the Schaffer collateral pathway in field CA1 in the rat hippocampal slice. *Neuroreport,* **8,** 745–749.

OTMAKHOVA, N.A. & LISMAN, J.E. (1999). Dopamine selectively inhibits the direct cortical pathway to the CA1 hippocampal region. *J. Neurosci.,* **19,** 1437–1445.

OTMAKHOVA, N.A. & LISMAN, J.E. (2000). Dopamine, serotonin, and noradrenaline strongly inhibit the direct perforant path-CA1 synaptic input, but have little effect on the Schaffer collateral input. *Ann. N.Y. Acad. Sci.,* **911,** 462–464.

OTMAKHOVA, N.A., OTMAKHOV, N. & LISMAN, J.E. (2002). Pathway-specific properties of AMPA and NMDA-mediated transmission in CA1 hippocampal pyramidal cells. *J. Neurosci.,* **22,** 1199–1207.

PHILPOT, B.D., SEKHAR, A.K., SHOUVAL, H.Z. & BEAR, M.F. (2001). Visual experience and deprivation bidirectionally modify the composition and function of NMDA receptors in visual cortex. *Neuron,* **29,** 157–169.

QUINLAN, E.M., PHILPOT, B.D., HUGANIR, R.L. & BEAR, M.F. (1999). Rapid, experience-dependent expression of synaptic NMDA receptors in visual cortex *in vivo*. *Nat. Neurosci.,* **2,** 352–357.

RUMBAUGH, G. & VICINI, S. (1999). Distinct synaptic and extrasynaptic NMDA receptors in developing cerebellar granule neurons. *J. Neurosci.,* **19,** 10603–10610.

SHI, J., AAMODT, S.M. & CONSTANTINE-PATON, M. (1997). Temporal correlations between functional and molecular changes in NMDA receptors and GABA neurotransmission in the superior colliculus. *J. Neurosci.,* **17,** 6264–6276.

STEWARD, O. (1976). Topographic organization of the projections from the entorhinal area to the hippocampal formation of the rat. *J. Comput. Neurol.,* **167,** 285–314.

STOCCA, G. & VICINI, S. (1998). Increased contribution of NR2A subunit to synaptic NMDA receptors in developing rat cortical neurons. *J. Physiol.,* **507** (Part 1), 13–24.

TANG, Y.P., SHIMIZU, E., DUBE, G.R., RAMPON, C., KERCHNER, G.A., ZHUO, M., LIU, G. & TSIEN, J.Z. (1999). Genetic enhancement of learning and memory in mice. *Nature,* **401,** 63–69.

TOVAR, K.R. & WESTBROOK, G.L. (1999). The incorporation of NMDA receptors with a distinct subunit composition at nascent hippocampal synapses *in vitro*. *J. Neurosci.,* **19,** 4180–4188.

VICINI, S., WANG, J.F., LI, J.H., ZHU, W.J., WANG, Y.H., LUO, J.H., WOLFE, B.B. & GRAYSON, D.R. (1998). Functional and pharmacological differences between recombinant *N*-methyl-D-aspartate receptors. *J. Neurophysiol.,* **79,** 555–566.

WATKINS, C.J., PEI, Q. & NEWBERRY, N.R. (1998). Differential effects of electroconvulsive shock on the glutamate receptor mRNAs for NR2A, NR2B and mGluR5b. *Brain. Res. Mol. Brain. Res.,* **61,** 108–113.

WILLIAMS, K. (1993). Ifenprodil discriminates subtypes of the *N*-methyl-D-aspartate receptor: selectivity and mechanisms at recombinant heteromeric receptors. *Mol. Pharmacol.,* **44,** 851–859.

WILLIAMS, K. (1995). Pharmacological properties of recombinant *N*-methyl-D-aspartate (NMDA) receptors containing the epsilon 4 (NR2D) subunit. *Neurosci. Lett.,* **184,** 181–184.

(Received November 20, 2003
Revised January 16, 2004
Accepted February 13, 2004)